ISET Journal of Earthquake Technology, Paper No. 468, Vol. 43, No. 1-2, March-June 2006, pp. 11-29

ANALYSIS OF STRONG MOTION DATA OF THE UTTARKASHI EARTHQUAKE OF 20TH OCTOBER 1991 AND THE CHAMOLI EARTHQUAKE OF 28TH MARCH 1999 FOR DETERMINING THE *Q* VALUE AND SOURCE PARAMETERS

Anand Joshi

Department of Geophysics
Kurukshetra University, Kurukshetra-136119

ABSTRACT

Analysis is presented in this paper to fit the theoretical S-wave acceleration spectra conditioned by frequency-independent *Q* with the observed acceleration spectra. The estimate of error is given in the root-mean-square sense over all the frequencies. The data of two major earthquakes in the Garhwal Himalayas, namely the 1991 Uttarkashi Earthquake and the 1999 Chamoli Earthquake, has been used in the present study to obtain source parameters of these earthquakes and *Q* value in the source region. Independent estimates of *Q* at various stations give its average value as 267±87. The stress drop for the Uttarkashi and the Chamoli earthquakes is computed as 77 and 29 bars, respectively, from the near-field acceleration spectra of BHAT and GOPE stations. This agrees with the other observed values of stress drop in the Himalayas.

KEYWORDS: Source Spectrum, Inversion, *Q*, Attenuation

INTRODUCTION

Acceleration spectrum is one of the most direct and common functions used to describe the frequency content of strong ground earthquake shaking (Hudson, 1962). An acceleration spectrum contains valuable information regarding the source and medium characteristics. The source spectrum of an earthquake can be approximated by the omega-square model (Brune, 1970), which has ω^2 decay of high frequencies above the corner frequency. The source acceleration spectrum can be estimated from an acceleration record after correcting it with diminution function, which accounts for the geometrical spreading and anelastic attenuation. The anelastic attenuation of seismic waves is characterized by a dimensionless quantity called quality factor *Q* (Knopoff, 1964).

Until today very few studies have been carried out to understand the attenuation characteristics of the Himalayan crust. Examples include the work by Gupta et al. (1995) and Mandal et al. (2001). Their work is based on the microtremor and aftershock data and thus contains information on the shallow crust. An analysis scheme for obtaining source parameters and quality factor *Q* using the least-square inversion technique has been presented in this paper. The work presented here is based on the technique of Fletcher (1995) that uses nonlinear least-square algorithm and Newton's method. In this paper the Brune's source model (Brune, 1970) is used together with the propagation filter.

This study uses the strong motion data of the Uttarkashi (M_s = 7.0) and the Chamoli (M_s = 6.6) earthquakes recorded by strong motion array maintained by the Department of Earthquake Engineering, Indian Institute of Technology Roorkee, India. The epicenters of these two earthquakes were close to each other and were in the same tectonic environment. The main objectives of this paper are: (i) to compute the source parameters of these two Himalayan earthquakes by using the strong motion data, and (ii) to compute the mid-crustal *Q* value in the Garhwal Himalayas.

INVERSION PROCEDURE

The acceleration spectrum of shear waves at distance R due to an earthquake of seismic moment M_o can be described by (e.g., Boore, 1983; Atkinson and Boore, 1998):

$$A(f) = CM_o\, S(f)\, D(f)\, R_s(f) \tag{1}$$

where C is a constant for a particular station; filter $S(f)$ represents the source acceleration spectrum; $R_s(f)$ denotes the site amplification factor; and $D(f)$ denotes the frequency-dependent diminution function (e.g., Boore and Atkinson, 1987):

$$D(f) = \frac{e^{-\pi fR/Q\beta} P(f, f_m)}{R} \tag{2}$$

In the above equation, $P(f, f_m)$ is a high-cut filter, and $e^{-\pi fR/Q\beta}/R$ is a propagation filter. The term f_m in the high-cut filter may be interpreted as attenuation near the recording site (Hanks, 1982), but for most recorded accelerograms, selection of f_m is governed by the signal-to-noise ratio at high frequencies and is usually set as 25 Hz (Trifunac and Lee, 1973). In the present work, f_m is kept as 25 Hz. The parameter $t^* = R/Q\beta$ is defined as attenuation time. If Q is independent of frequency, the form of attenuation function will be as in the κ model (Trifunac, 1994; Anderson and Hough, 1984). By introducing t^*, Equation (1) is rewritten as

$$A(f) = \frac{CS(f)e^{-\pi t^* f} R_s(f)}{R} \tag{3}$$

This expression serves as the basis for our analysis. In this expression, C is constant for any site for a given earthquake and for a double couple embedded in an elastic medium, while considering only S waves. It is given as (Boore, 1983)

$$C = \frac{M_o R_{\theta\phi}\, FS\, PRTITN}{4\pi\rho\beta^3} \tag{4}$$

where $R_{\theta\phi}$ is the radiation pattern; M_o is the seismic moment; FS is the amplification due to the free surface; $PRTITN$ is the reduction factor that accounts for partitioning of energy into two horizontal components; and ρ and β are density, and the shear wave velocity, respectively. The filter $S(f)$ defines the source spectrum of the earthquake under consideration. In the present work, we follow the spectrum defined by Brune (1970) and therefore consider

$$S(f) = \frac{(2\pi f)^2}{1 + (f / f_c)^2} \tag{5}$$

where f_c is the corner frequency, and $f_c = 2.34\beta / 2\pi r_o$ with r_o denoting the radius of the equivalent earthquake source. The exponential term in Equation (1) explains the decay of acceleration spectrum with distance due to the anelastic attenuation and scattering. As the data used in the present analysis scheme is from the short distances, and because both earthquakes are shallow earthquakes with most of the energy confined to the uppermost layer of the crust, the quality factor will be assumed to be constant and independent of frequency (Sriram and Khattri, 1997). Fletcher (1995) has also used a frequency-independent Q value as it fitted well with his dataset (see also Boatwright et al., 1991; Atkinson and Mereu, 1992). There are some independent evidences in conjunction with the seismic exploration technique that indicate that Q can be approximated by a constant value in the shallow crust (Knopoff, 1964; Tullos and Reid, 1969; Trifunac, 1994; Hamilton, 1972, 1976; Ganley and Kanasewich, 1980; Hauge, 1981; McDonal et al., 1958). As the Himalayan earthquakes have been occurring in the shallow crust, the assumption of frequency-independent Q will be made here.

Equation (1) serves as the basic equation for our analysis. We linearize it by taking its natural logarithm:

$$\ln A(f) = \ln C + \ln S(f) - \pi t^* f - \ln R + \ln R_s(f) + \varepsilon \tag{6}$$

where t^* and ε are unknown parameters. The parameter ε is introduced to account for the error in the computations. The term representing the source filter $S(f)$ can be replaced with its expression in Equation (5). For a known value of f_c, the two unknowns, Q and ε, can be obtained from inversion by minimizing in the least-square sense, whereas the value of f_c is chosen in an iterative manner. The least-square inversion minimizes

$$\chi^2 = \sum [A_s(f) - S(f)]^2 \tag{7}$$

where $S(f)$ is the source acceleration spectrum as proposed by Brune (1970). For the purpose of analysis, we rearrange Equation (6) in the following form:

$$\ln M_o - \pi f t^* = \ln A(f) - \ln C - \ln S(f) + \ln R - \ln R_s(f) + \varepsilon \tag{8}$$

This leads to the following set of equations for frequencies $f_1, f_2, f_3, ..., f_n$, where n denotes the total number of samples in the acceleration record:

$$\begin{aligned} \varepsilon - \pi f_1 t^* &= DA(f_1) \\ \varepsilon - \pi f_2 t^* &= DA(f_2) \\ \varepsilon - \pi f_3 t^* &= DA(f_3) \\ &\ldots\ldots\ldots\ldots \\ \varepsilon - \pi f_n t^* &= DA(f_n) \end{aligned} \tag{9}$$

with

$$DA(f_i) = \ln A(f_i) - \ln C - \ln S(f_i) + \ln R \tag{10}$$

In matrix form Equations (9) can be written as

$$\begin{bmatrix} 1 & -\pi f_1 \\ 1 & -\pi f_2 \\ 1 & -\pi f_3 \\ \vdots & \vdots \\ 1 & -\pi f_n \end{bmatrix} \begin{bmatrix} \varepsilon \\ t^* \end{bmatrix} = \begin{bmatrix} DA(f_1) \\ DA(f_2) \\ DA(f_3) \\ \vdots \\ DA(f_n) \end{bmatrix} \tag{11}$$

The above expression provides a basic statement of the following problem in which the model parameters and the data are in some way related to each other (Menke, 1984):

$$Gm = d \tag{12}$$

Here, G represents the rectangular matrix, m the model matrix, and d the data matrix. Inversion of G gives the following model matrix:

$$m = (G^T G)^{-1} G^T d \tag{13}$$

This inversion is prone to problems if $G^T G$ is close to being singular, and for such a case, singular value decomposition (SVD) is used to solve for m (Press et al., 1993). Our formulation of SVD follows Lancose (1961). In this formulation the G matrix is decomposed into U_p, V_p and A_p matrices as (Fletcher, 1995)

$$G^{-1} = V_p A_p U_p^T \tag{14}$$

where V_p, U_p and A_p have nonzero eigenvectors and eigenvalues. Our technique differs from that of Fletcher (1995) as acceleration spectrum has been used to obtain t^* from the independent estimates of f_c and M_o. The entire scheme of analysis for obtaining t^* is shown in Figure 1 in the form of a flow-chart.

DATA-SET

Under a project funded by the Department of Science and Technology, Government of India, the Department of Earthquake Engineering, Indian Institute of Technology Roorkee maintains a network of strong motion stations in the Uttaranchal region of the Himalayas. This network is equipped with three component SMA-1 accelerographs. These are triggered accelerographs with recording on 70 mm film. The analogue records have been converted into digital records as described in Chandrasekaran and Das (1992). This array has recorded two recent earthquakes in this region, namely the Uttarkashi Earthquake of 20th October, 1991 and the Chamoli Earthquake of 28th March, 1999. The parameters of these two earthquakes are listed in Table 1.

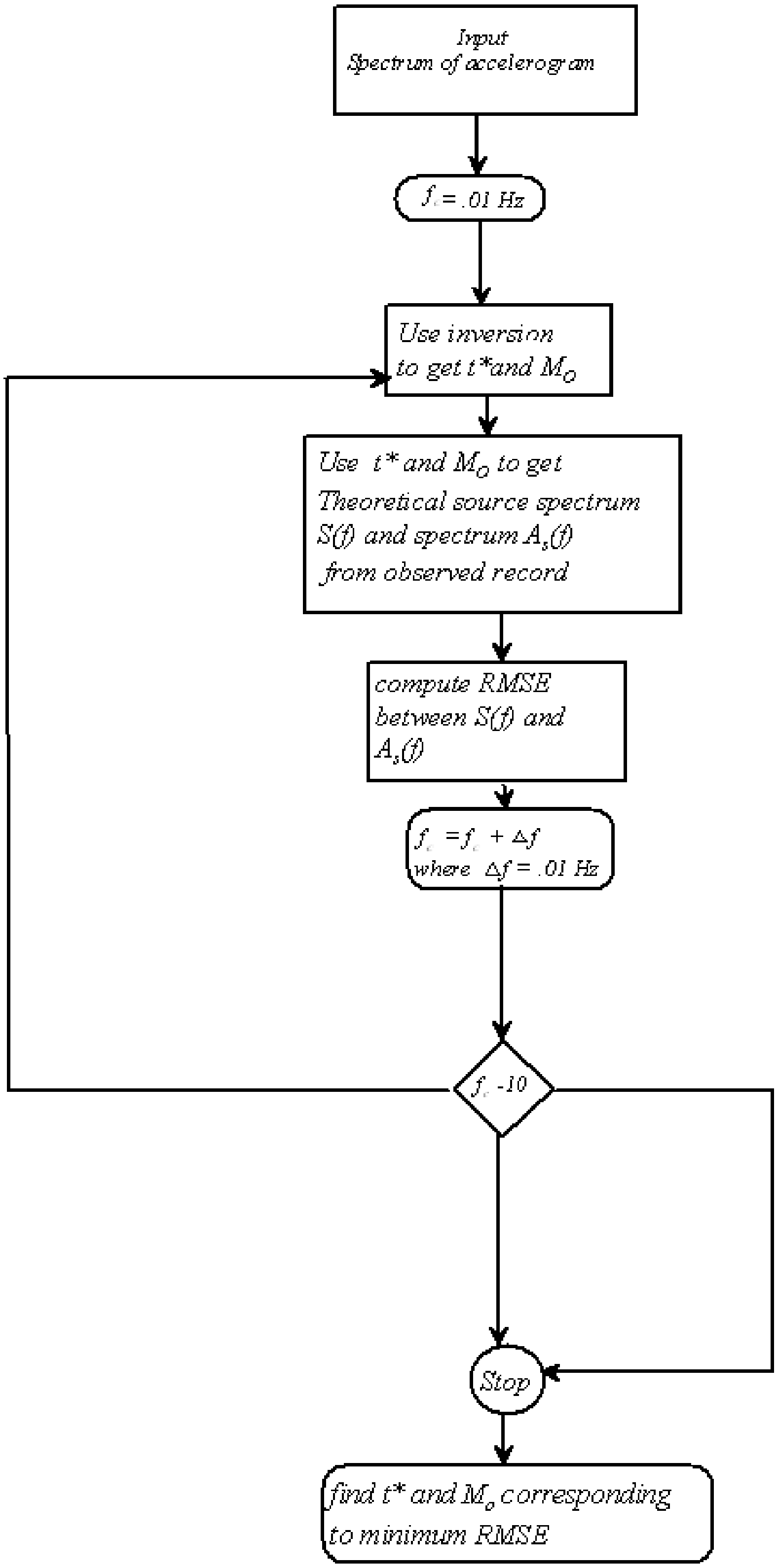

Fig. 1 Flow-chart of the entire process of inversion; the source model is that given by Brune (1970)

Table 1: Parameters of the Uttarkashi Earthquake of 20th October, 1991 and the Chamoli Earthquake of 28th March, 1999

Hypocenter	Size Source	Fault Plane Solution	Reference
Uttarkashi Earthquake			
21:23:14.3 (GMT) 30.78^{0}N, 78.77^{0}E 10 km	m_b = 6.5, M_s = 7.0 M_O = 1.80×10^{26} dyne-cm M_w = 6.8	$NP1$: φ = 296^0, δ = 5^0, λ = 90^0 $NP2$: φ = 116^0, δ = 85^0, λ = 90^0	PDE, Monthly
21:23:21.6 (GMT) 30.22^{0}N, 78.24^{0}E 15 km	M_w = 6.8 M_O = 0.80×10^{26} dyne-cm	$NP1$: φ = 317^0, δ = 14^0, λ = 115^0 $NP2$: φ = 112^0, δ = 78^0, λ = 84^0	CMT (Harvard)
Chamoli Earthquake			
19:05:11.0 (GMT) 30.51^{0}N, 79.40^{0}E 15 km	m_b = 6.4 M_s = 6.6 M_O = 1.80×10^{26} dyne-cm	$NP1$: φ = 282^0, δ = 9^0, λ = 95^0 $NP2$: φ = 97^0, δ = 81^0, λ = 89^0	USGS
19:05:18.1 (GMT) 30.38^{0}N, 79.21^{0}E 15 km	m_b = 6.4, M_s = 6.6 M_w = 6.5 M_O = 7.77×10^{25} dyne-cm	$NP1$: φ = 280^0, δ = 7^0, λ = 75^0 $NP2$: φ = 115^0, δ = 83^0, λ = 92^0	CMT (Harvard)

In the present work digital acceleration records processed from the analogue records have been used. The correction and filtering procedures used for processing (Lee and Trifunac, 1979) are described in Chandrasekaran and Das (1992). The data-sampling rate is 0.02 sec, and the data has been band-pass filtered by using Ormsby filter. The specifications of the Ormsby filter used for processing of the records of the Chamoli Earthquake are given in Table 2. The filter settings for the records of the Uttarkashi Earthquake are same for all stations, with the low- and high-filter settings as 0.17-0.20 and 25-27 Hz, respectively. Due to these filters, used in the processing of the acceleration data, it became difficult to determine the corner frequency. Further, as the triggered recording mode is used in the instruments, at many stations their records with unclear starting phase were seen. This made it difficult to clearly identify the S-phase of those records. Clear identification of the S-phase was possible at five stations for the Uttarkashi Earthquake and five for the Chamoli Earthquake. Stations lying within 60 km distance range are usually dominated by the direct shear waves. Beyond this distance, the post-critical reflection from Moho and a layer within the crust, and the L_g phases contribute significantly to the strong ground motion (Sriram and Khattri, 1997). Due to this reason only four stations have been retained for the analysis. The other stations lie at distances greater than 60 km. The selected stations are located mostly along the trend of Main Central Thrust (MCT), and lie in the Lesser Himalayan sequence except BHAT that lies in the Higher Himalayan sequence (Figures 2 and 3).

Table 2: Filtering Specifications of the Processed Accelerograms Recorded during the Chamoli Earthquake

Station	Epicentral Distance (km)	Filtering Parameters of			
		L-Component (Hz)		T-Component (Hz)	
GOPE	22	0.110-0.130	25-27	0.080-0.100	25-27
JOSH	29	0.400-0.550	25-27	0.175-0.225	25-27
GHAN	77	0.300-0.400	25-27	0.425-0.525	25-27
TEHR	91	0.200-0.250	25-27	0.175-0.225	25-27

Both of the earthquakes considered in this study had shallow focus, occurring in the basement thrust (Jain and Chander, 1995; Joshi, 2000, 2001; Joshi et al., 2001). The Uttarkashi Earthquake was recorded at thirteen stations while the Chamoli Earthquake was recorded at nine. Locations of all stations that had recorded these two earthquakes are shown in Figure 2. Locations of the stations used in the analysis in this paper are shown in Figure 3, together with the geology and tectonics of the area. Site conditions seen from the geological map show that most of the sites are in a high Himalayan mountain terrain and in the meta-sedimentary Lesser Himalayan province, which is expected to be devoid of thick sedimentary cover. However, they could be on sediments in the river valley or on severely fractured and weathered rock. Among these stations, only Bhatwari is located on the central crystalline province of the Higher Himalayas. It can be seen from Figure 3 that most of the selected stations are located in the Lesser Himalayan region. The Lesser Himalayas consist of the sediments of the Precambrian-Palaeozoic age, and locally of the Mesozoic age, metamorphosed and subdivided by thrusts with progressively older rocks toward the north (Sharma and Wason, 1994). The Lesser Himalayas have been thrust southwards over the Siwaliks of the Sub-Himalayas along the Main Boundary Thrust (MBT). The northern boundary of the Lesser Himalayas is defined by the MCT. This separates it from the Higher Himalayas. Historically earthquakes have been recorded in the region between the MBT and the MCT (Seeber and Armbruster, 1984). The fault mechanism of the 1905 Kangra Earthquake and the fault plane solutions of the 1979 Dharchula Earthquake, 1991 Uttarkashi Earthquake, and 1999 Chamoli Earthquake showed that the dominant deformation model for the region is low-angle northeasterly dipping thrust faulting (Thakur and Kumar, 2002). Khattri et al. (1989) indicated that moderate earthquakes occur in this region due to the reactivation of the low-angle thrust faults in the upper crust parallel to the detachment surface. These earthquakes have been discussed in terms of reactivation of upper crustal faults, which are possibly slip surfaces of crustal shear zones facilitating the uplifting of Lesser as well as Higher Himalayas, and are a consequence of the same underthrusting Himalayan orogenic process prevalent in the entire region (Mandal et al., 2001).

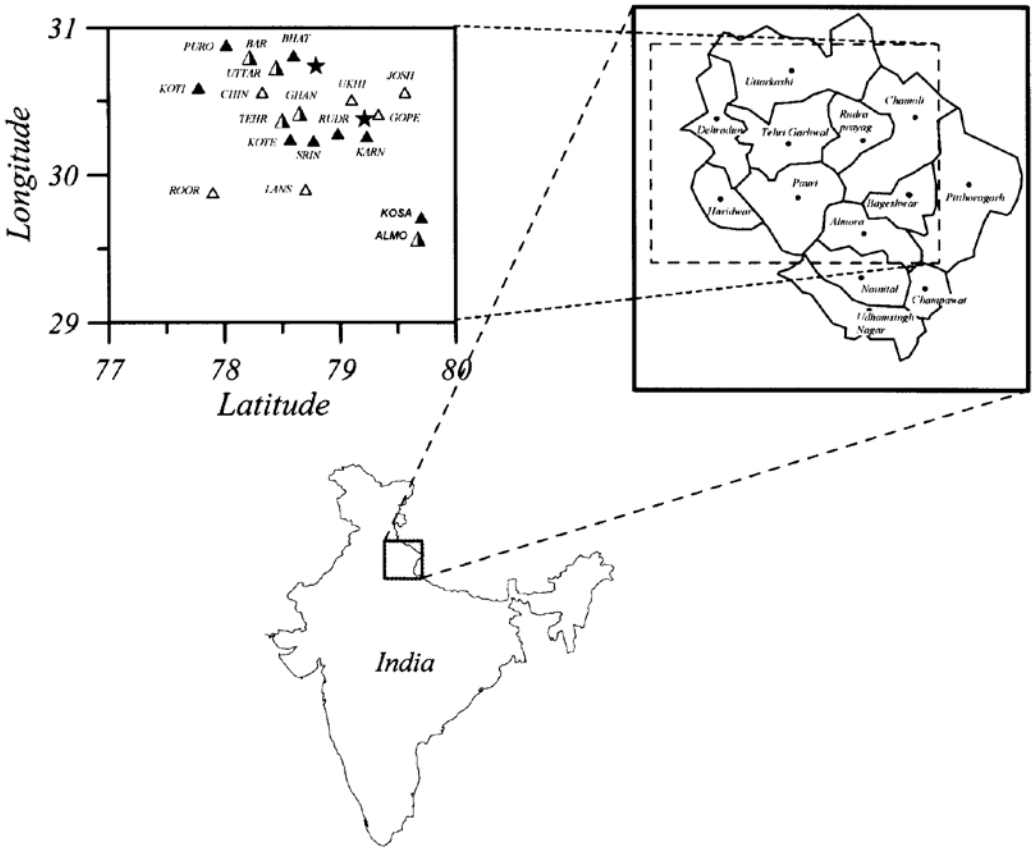

Fig. 2 Locations of all stations that had recorded the Uttarkashi and Chamoli earthquakes (the black triangles denote the locations of those stations that had recorded the Uttarkashi Earthquake, the empty triangles denote the locations of those stations that had recorded the Chamoli Earthquake, and the half-filled triangles denote the locations of those stations that had recorded both Uttarkashi and Chamoli earthquakes; the stars denote the epicenters of the Uttarkashi and Chamoli earthquakes)

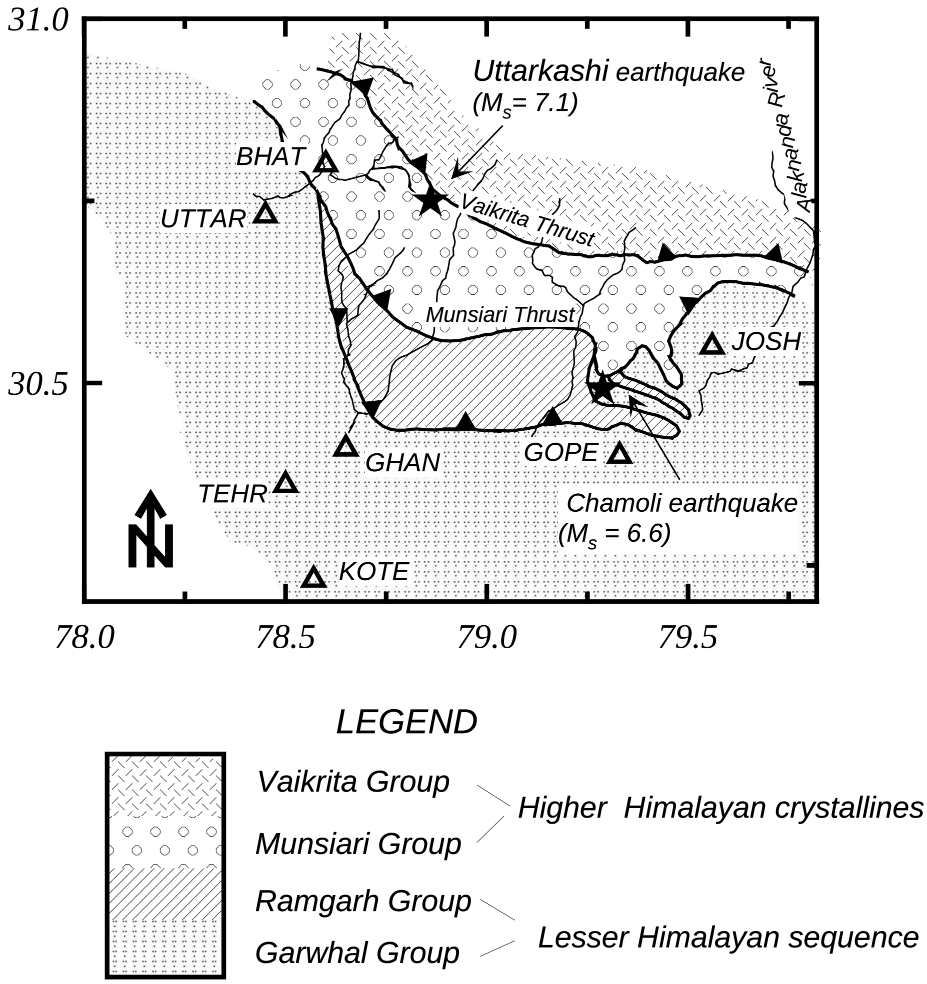

Fig. 3 Tectonics of the region surrounding the epicenters of the Chamoli and Uttarkashi earthquakes (after Metcalfe (1993)); locations of the stations that are used in the inversion process are shown by the triangles; stars denote the epicenters of the Uttarkashi and Chamoli earthquakes

An upward increase in the metamorphic grade across the Himalayas has been noticed by various geologists (Mallet, 1874; Medlicott, 1864; Oldham, 1883; Hodges et al., 1996; Pêcher, 1975; Stephenson et al., 2000). The inverted gradient is most obvious within and close to the MCT zone (Bollinger et al., 2004), which marks the contrast between the High Himalayan Crystalline (HHC) unit and the Lesser Himalayas. This observation has been interpreted due to the thermal structure with recumbent isotherms (Le Fort, 1975). The metamorphic and exhumation history of Lesser Himalayas remains poorly documented due to the poor mineralogy of these rocks and supposedly low metamorphic grade (Bollinger et al., 2004). Based on the data of Lesser Himalayas it is estimated that peak metamorphic temperatures decrease gradually from 520°-550°C below MCT zone down to less than 330°C. These temperatures describe structurally a 20°-50°C/km inverted exhumation history of Lesser Himalayas, thus supporting the view that since the Miocene, the Himalayan orogen has essentially grown by underplating rather than by frontal accretion (Bollinger et al., 2004). The thermal structure of the Himalayan orogen is consistent with the metamorphic rock exhumed from the Himalayas, and has temperature of 0°C at the earth surface and a constant mantle heat flow of 15 mW/m^2 at the base of the model. The upper crust heat production is taken to be 25 W/μm^3 (Cattin et al., 2001). The computed thermal structure of the Indian plate away from the Himalayas implies a surface heat flow of about 60 mW/m^2, which is consistent with the measurement made in the cratonic areas of northern India (Pandey and Agrawal, 1999). This model suggests that density of the Himalayan crust might not be uniform due to the thermal structure and possible petrological changes related to the underthrusting of the Indian crust (Le Pichnon et al., 1997; Henry et al., 1997).

RESULTS OF INVERSION

The first step in the analysis is the identification of S-phase from the available strong motion data. Because of the threshold level of 0.01*g* as the triggering level of the strong motion recordings it is difficult to say whether a record actually started after arrival of the P-phase or from the S-phase, especially in the case of less energetic motions. We have taken those stations at which we can identify S-phase visually after zooming onto the portion before the onset of S-phase. Four stations in the case of the Chamoli earthquake and four in the case of the Uttarkashi earthquake have been selected for the analysis. Our procedure gives t^* for the case of the Brune's source model. The obtained t^* value is used to compute the source spectrum at each station from the digitized accelerogram. In the present work analysis has been made for $R_s(f) = 1.0,$ i.e., without considering the site effects. Sriram and Khattri (1997) and Singh et al. (2002) have estimated the corner frequency for the Uttarkashi and the Chamoli earthquakes as 0.08 Hz and 0.13 Hz, respectively. The seismic moment has been assumed as 1.80×10^{26} and 2.77×10^{26} dyne-cm for the Uttarkashi and Chamoli earthquakes, respectively, as given by USGS. By using these values of corner frequency and seismic moment, inversion is performed to obtain t^*. Tables 3 and 4 give the values of *Q* obtained after the inversion at different stations. The source spectrum and the corresponding Brune's model obtained at different stations are shown in Figures 4-7.

Table 3: Results of Inversion of the Strong Motion Data of the Chamoli Earthquake

Station Name	Station Code	*R* (km)	Component	*Q*	Root-Mean-Square Error
Gopeshwar	GOPE	19	Longitudinal (L)	95	0.085
			Transverse (T)	112	0.115
Joshimath	JOSH	41	Longitudinal (L)	351	0.430
			Transverse (T)	342	0.111
Ghansiali	GHAN	55	Longitudinal (L)	305	0.061
			Transverse (T)	263	0.154
Tehri	TEH	69	Longitudinal (L)	361	0.082
			Transverse (T)	341	0.430

Table 4: Results of Inversion of the Strong Motion Data of the Uttarkashi Earthquake

Station Name	Station Code	*R* (km)	Component	*Q*	Root-Mean-Square Error
Uttarkashi	UTTAR	41	Longitudinal (L)	213	0.032
			Transverse (T)	219	0.027
Bhatwari	BHAT	28	Longitudinal (L)	185	0.028
			Transverse (T)	195	0.215
Ghansiali	GHAN	43	Longitudinal (L)	259	0.119
			Transverse (T)	238	0.024
Koteshwar	KOTE	63	Longitudinal (L)	328	0.024
			Transverse (T)	378	0.024

As the corner frequency obtained for the Uttarkashi and Chamoli earthquakes is outside the frequency-band of the processed accelerograms, it is not visible in the comparisons shown in Figures 4-7. Another corner is seen around 1.0 Hz and 0.8 Hz in the source spectra of the Chamoli and Uttarkashi earthquakes respectively. A departure from the simple Brune model may be expected for large earthquakes for which the single corner frequency representation is unrealistic (Atkinson and Silva, 1997). The factors, that result in more that one corner frequency in the source spectrum of a large earthquake, include the elongated rupture, as opposed to the circular one (Savage, 1972), partial stress drop (Brune, 1970), and fault roughness (Gusev, 1983), interpreted as either barrier (Papageorgiou and Aki, 1983) or asperities (Kanamori and Stewart, 1978; Rudnicki and Kanamori, 1981). Due to these factors a single-corner-frequency point source consistently over-predicts ground motions at low-to-intermediate frequencies (~ 0.1-2 Hz) for moderate-to-large earthquakes (Atkinson and Silva, 2000;

Boatwright and Choy, 1992; Boore and Atkinson, 1992; Atkinson, 1993; Atkinson and Boore, 1998; Atkinson and Silva, 1997). Such two-corner-frequency source spectra have been also reported by Sriram and Khattri (1997) for the Uttarkashi Earthquake and explained in terms of the two-corner Atkinson's model (Atkinson, 1993). The Brune's spectrum allows a better fit beyond 2 Hz frequencies at nearly all stations.

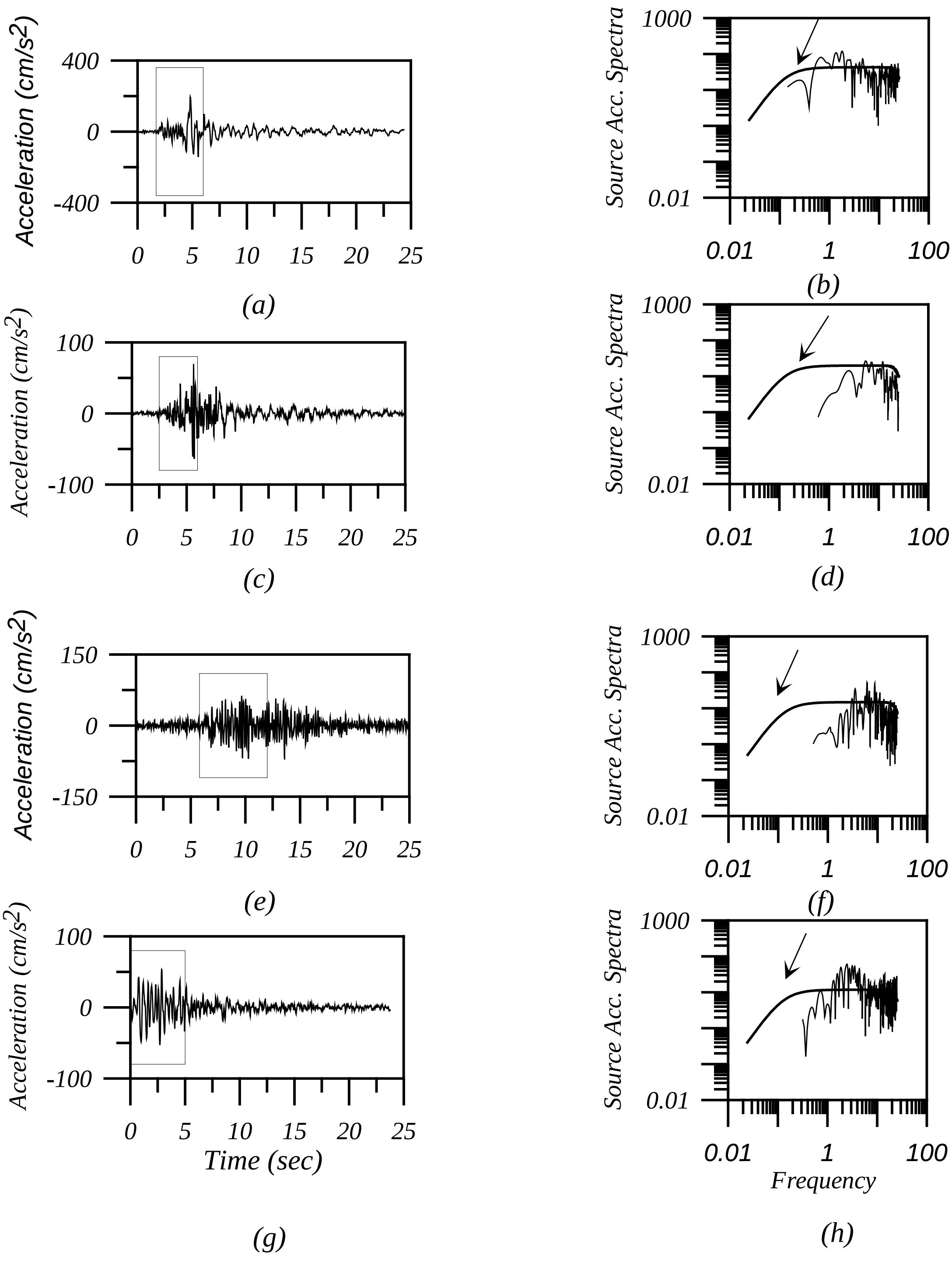

Fig. 4 Selected portions of the longitudinal component of the accelerograms of the Chamoli Earthquake, as used for the inversion, and comparisons of the source spectra from the actual records and those from the Brune's model (see the acceleration records at (a) GOPE, (c) JOSH, (e) GHAN and (g) TEH stations, and the source spectra at (b) GOPE, (d) JOSH, (f) GHAN and (h) TEH stations); the thick solid line shows the theoretical Brune's spectrum, and the spectrum from the observed record is shown by the thin dark line

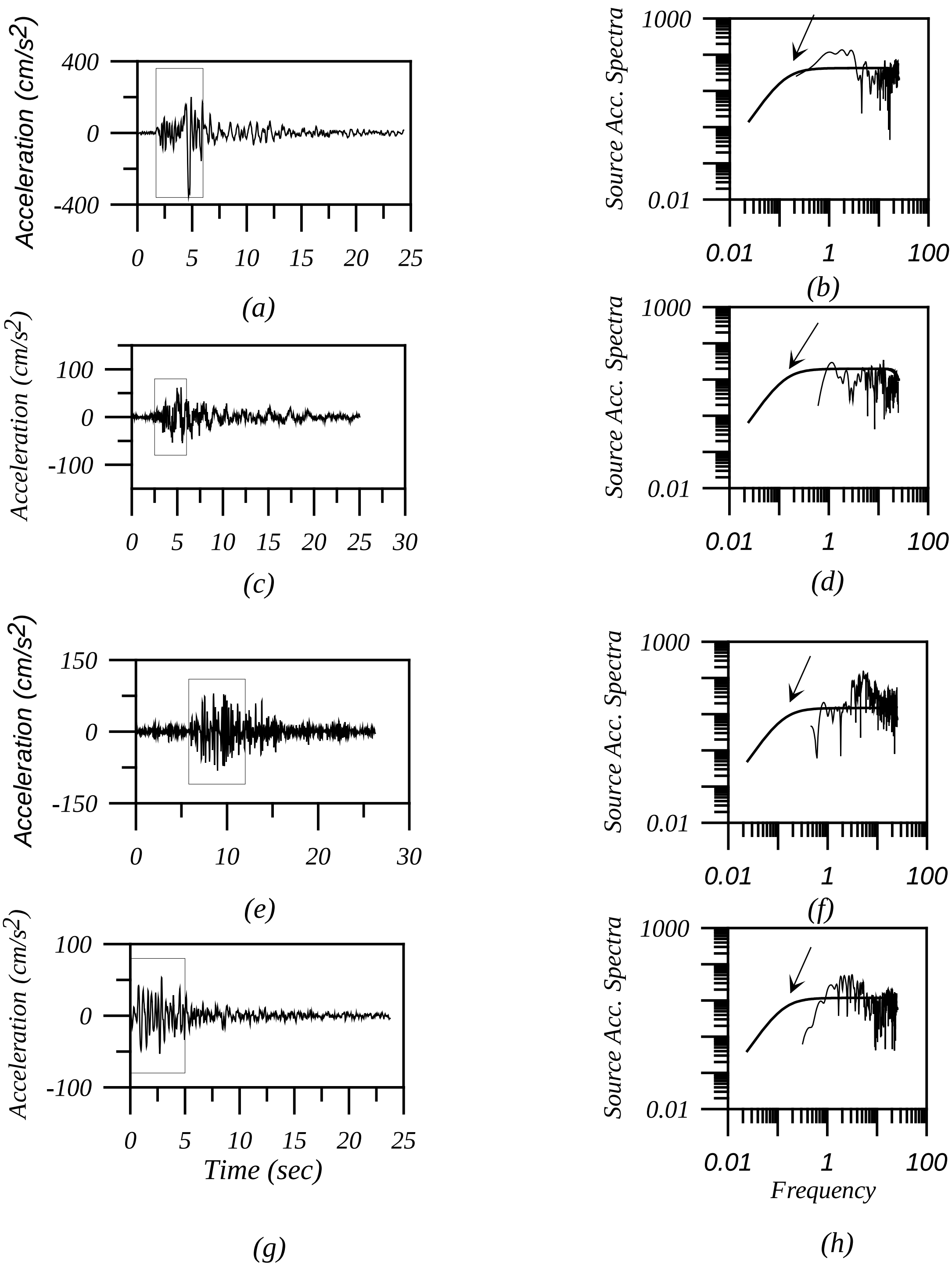

Fig. 5 Selected portions of the transverse component of the accelerograms of the Chamoli Earthquake, as used for the inversion, and comparisons of the source spectra from the actual records and those from the Brune's model (see the acceleration records at (a) GOPE, (c) JOSH, (e) GHAN and (g) TEH stations, and the source spectra at (b) GOPE, (d) JOSH, (f) GHAN and (h) TEH stations); the thick solid line shows the theoretical Brune's spectrum, and the spectrum from the observed record is shown by the thin dark line

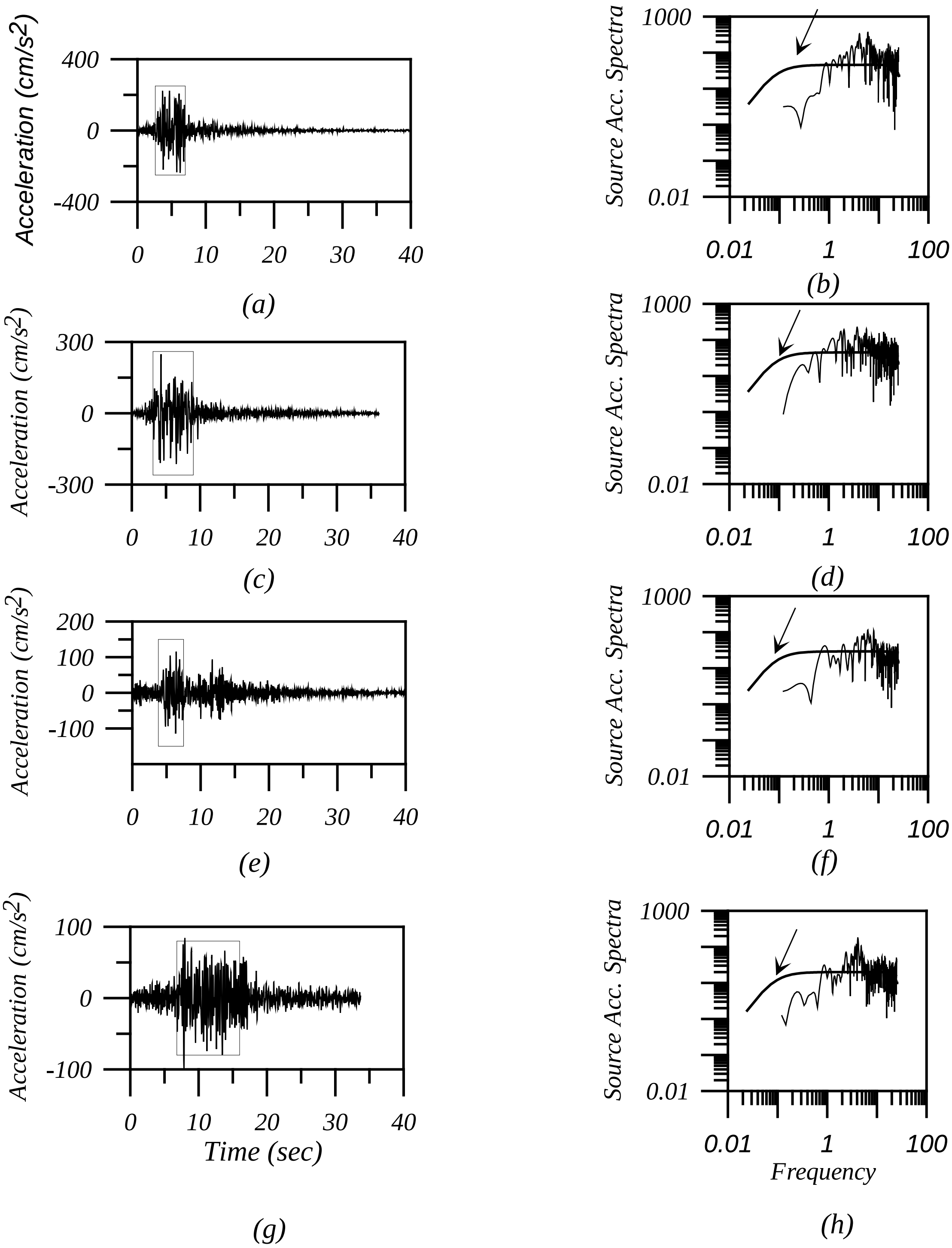

Fig. 6 Selected portions of the longitudinal component of the accelerograms of the Uttarkashi Earthquake, as used for the inversion, and comparisons of the source spectra from the actual records and those from the Brune's model (see the acceleration records at (a) UTTAR, (c) BHAT, (e) GHAN and (g) KOTE stations, and the source spectra at (b) UTTAR, (d) BHAT, (f) GHAN and (h) KOTE stations); the thick solid line shows the theoretical Brune's spectrum, and the spectrum from the observed record is shown by the thin dark line

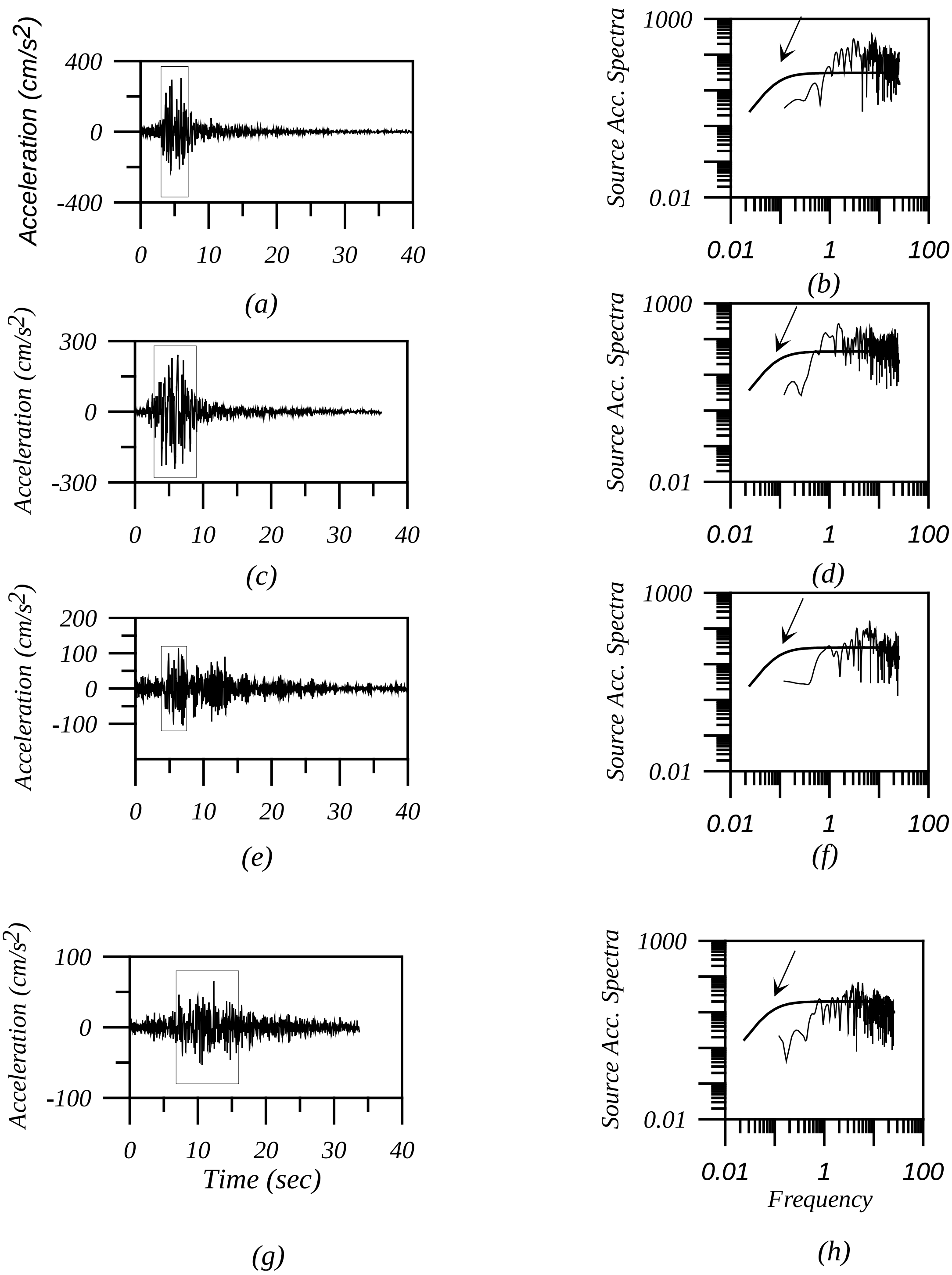

Fig. 7 Selected portions of the transverse component of the accelerograms of the Uttarkashi Earthquake, as used for the inversion, and comparisons of the source spectra from the actual records and those from the Brune's model (see the acceleration records at (a) UTTAR, (c) BHAT, (e) GHAN and (g) KOTE stations, and the source spectra at (b) UTTAR, (d) BHAT, (f) GHAN and (h) KOTE stations); the thick solid line shows the theoretical Brune's spectrum, and the spectrum from the observed record is shown by the thin dark line

It may be mentioned that the parameter representing the source is its size, which is defined in this study by the radius of circular rupture. The radius r_o of this equivalent circular crack is related to the corner frequency f_c of the source spectrum and is calculated following the relation given by Brune (1970, 1971):

$$r_o = \frac{2.34\beta}{2\pi f_c} \tag{15}$$

DISCUSSION

In this study, the attenuation time t^* is obtained from the analysis of strong motion data. This parameter is related to the attenuation characteristics of the medium. We now focus on two important aspects of this study, one related to the source model and other to the Q value of the region.

1. Source Model

The analysis of the strong motion acceleration data has been performed using the model of Brune (1970). Frequency characteristics of this model depend on the corner frequency. As corner frequency is related to the source size, several possibilities were checked, and based on the comparison of the root-mean-square (RMS) error, it has been seen that 0.16 Hz and 0.09 Hz are the best estimates for the Chamoli Earthquake and the Uttarkashi Earthquake respectively. Using these corner frequencies, analysis of the acceleration spectra, corrected for the site effects, has been performed and seismic moment has been obtained at different stations. Using the relationship between the corner frequency and the source radius as given in Equation (15), the source radius for the Uttarkashi and Chamoli earthquakes is calculated as 13.2 km and 7.4 km, respectively. Aftershock distributions of the two earthquakes are shown in Figure 8, together with the projections of the approximately circular ruptures. Figure 8 shows that in each case, most of the aftershocks fall within the estimated rupture area of the main shock.

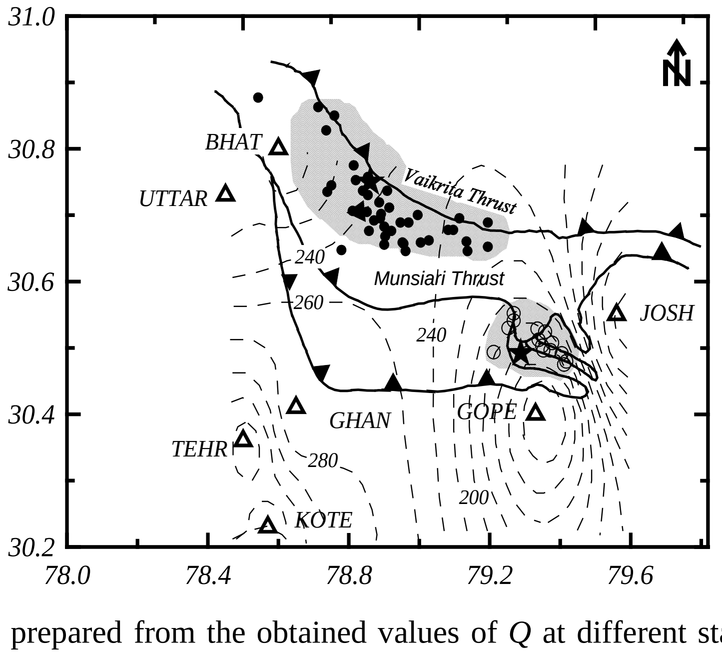

Fig. 8 Contours of Q prepared from the obtained values of Q at different stations on tectonic map of the region (shaded circles show the rupture areas of the two earthquakes; shaded regions show the aftershock areas; the aftershock data of the Uttarkashi Earthquake is taken from Kayal et al. (1995) and that of the Chamoli Earthquake from Mandal et al. (2001))

Using dislocation model of Brune (1970), the near-field S-wave acceleration spectrum may be approximated as (Trifunac, 1972a)

$$S_{NF}(f) = \frac{\sigma\beta(2\pi f)}{\mu\left[(2\pi f)^2 + \tau^{-2}\right]^{1/2}} \tag{16}$$

where σ is the effective stress, β is the shear wave velocity, μ is the modulus of rigidity, and $\tau \approx r/\beta$, with *r* representing the radius of equivalent circular dislocation surface. In the present work the stress drop has also been computed using the approach given by Trifunac (1972a, 1972b) from the spectrum of the near-field acceleration record. The near-field records of the GOPE and BHAT stations, which have recorded the Chamoli and Uttarkashi earthquakes, respectively, have been used for this purpose. Fourier spectra of the accelerograms at these stations have been corrected for the attenuation along the propagation path and for the free-surface effects. Those have been then approximated by the theoretical spectra of the near-field acceleration records as in Equation (16). Figure 9 gives the comparisons of the theoretical and observed acceleration spectra due to S waves at GOPE and BHAT stations. Using $\beta = 3.2$ km/s and $\mu = 2.7 \times 10^{11}$ dyne/cm^2, effective stresses for the Uttarkashi and Chamoli earthquakes are estimated as 77 bars and 29 bars, respectively. The study by Yu et al. (1995) has estimated the stress drop to be 30 bars for the Uttarkashi Earthquake, while there has been no study regarding the stress drop computation of the Chamoli Earthquake.

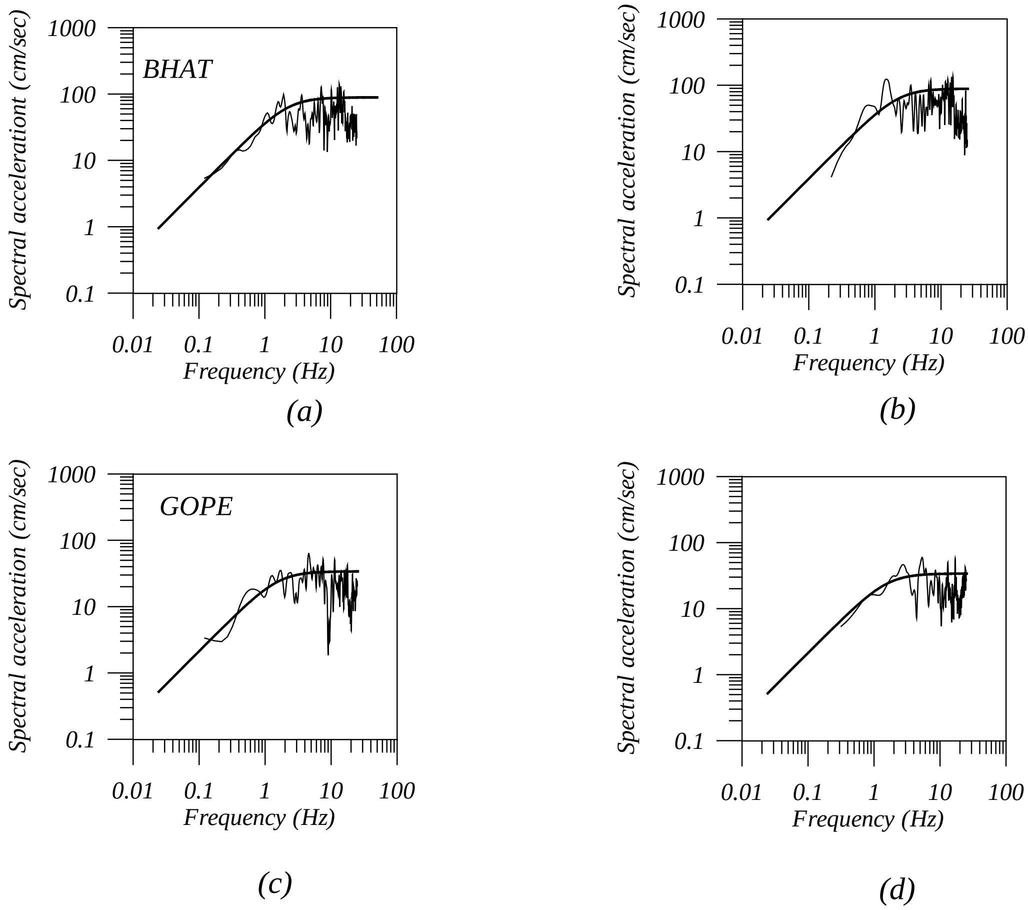

Fig. 9 Fourier amplitude spectra of near-field ground accelerations computed from the (a) longitudinal, (b) transverse components of acceleration records at BHAT, and (c) longitudinal, and (d) transverse components of acceleration records at GOPE stations; the theoretical spectra are shown by the thin lines

2. *Q* Value

For the Himalayan region, so far not much research has been done to get the estimates of *Q* values. Coda Q_c was determined by Mandal et al. (2001), using the 48 local aftershocks of the Chamoli Earthquake, which occurred within a circular area of 140 km radius. Magnitudes of the studied aftershocks ranged from 2.5 to 4.8. The average Q_o value was estimated to be of the order of 30±0.8. Based on the coda Q_c estimation using seven local earthquakes recorded in a network in the southwestern part of the Garhwal Himalayas, Gupta et al. (1995) suggested a frequency-dependent coda Q_c relation: $Q_c = 126f^{0.95}$, with less pronounced attenuation at higher frequencies. Different values of frequency-independent Q have been used by different studies on the source characteristics of Himalayan earthquakes (Sharma and Wason, 1994; Kumar and Khattri, 1999; Sriram and Khattri, 1997). Sharma and Wason (1994) used the Q value of the order of 300 in the Garhwal Himalayan region for the estimation of source parameters of earthquakes in the Garhwal Himalayas. Based on the 1988 Nepal-India Border Earthquake, the average quality factor Q_s has been estimated as 1310±158 by Kumar and Khattri (1999). As indicated by Kumar and Khattri (1999), this value is expected to be closely representative of the Himalayan region as well. Based on the model given by Yu et al. (1995), a constant Q of 1000 has been assumed by Sriram and Khattri (1997). Different values of Q have been obtained for different regions worldwide based on different locations and data. Tullos and Reid (1969) found severe attenuation corresponding to $Q_\alpha \sim 2$ over the depth range of 1-10 ft in the Gulf Coast sediments, 20 miles south of Houston. The attenuation was 1 to 2 orders of magnitude less severe at depths from 10 to 100 ft. Thouvenot (1983) reported that Q_α increases from 40, near the surface, to 600 at 7 km depth in a granite terrain in Central France. High Q is expected for the rocks like granite and basalt and can be around 1000, while it can be around 10 for soil and sediments near surface (Trifunac, 1994). Assuming no frequency dependence, Q of the order of 380 was obtained for the epicentral region of the aftershocks of the Loma Prieta Earthquake (Boatwright et al., 1991). A comparative study of Q_c value for many seismically active sites worldwide suggests low Q_c value for the sites like Guerrero (Mexico), Yugoslavia, Hindukush, and Parkfield (USA) (Rodriguez et al., 1983; Rovelli, 1984; Roecker et al., 1982; Hellweg et al., 1995).

The present study estimates average Q value as 267±87 using the strong motion data of two recent Himalayan earthquakes. It is rather difficult to check which of the estimates of Q, given by different researchers, is closer to reality as there are no means available for comparison directly or indirectly with the earlier studies. The method presented in this paper has an advantage that the obtained t^* values can be checked by computing the corresponding source acceleration spectra and by comparing those with the theoretical spectrum. The fit of observed spectra with the theoretical spectrum in terms of low RMS error demonstrates the efficacy of our approach and reliability of the obtained Q value. The value of computed RMS error at each station is given in Tables 3 and 4. At each station two values of Q are obtained. A contour map of average Q obtained at each station is shown in Fig. 8. It shows that the region covering higher Himalayan crystalline zone is characterized by low Q contours. At GOPE station low Q of about 95 is obtained which may be due to the highly attenuating characteristics of medium between the source and GOPE station. The tectonics of the region shows that the region surrounding GOPE station consists of highly complex shear zone MCT and its splays, which change their strike abruptly in this region. Singh et al. (1982) have also observed such low Q in the fault zone of Imperial Fault in California. In the region away in the southward direction from the MCT, high Q is observed which indicates the presence of a less attenuating medium. The second smallest value of Q of about 185 is obtained at BHAT station, which lies on the central crystalline province of Higher Himalayas. The values of Q obtained at all other stations are similar, and the reason for this is that they are located on similar tectonic and geological units. At GHAN station strong motion records of both earthquakes are available with clear S phase. Inversion of the spectra of all acceleration data at this station gives an estimate of Q, which is approximately same for all records. This suggests that the Q values, as obtained from the present inversion, are independent of the earthquake source and depend on the station at which the records are taken.

CONCLUSIONS

We have used the strong motion data of two recent Himalayan earthquakes, viz. the Uttarkashi Earthquake and the Chamoli Earthquake, to get the source parameters and quality factor Q. The analysis scheme presented in this paper is a modification of the scheme by Fletcher (1995). Inversion of the acceleration spectra has given the source parameters and the Q value in the source region. The stress drop values for the Uttarkashi and Chamoli earthquakes have been computed as 77 and 29 bars from the near-field acceleration spectra at BHAT and GOPE stations. This agrees with the other observed values of stress drop in the Himalayas.

ACKNOWLEDGEMENTS

The author sincerely acknowledges the use of the strong motion data collected by the Department of Earthquake Engineering, Indian Institute of Technology Roorkee, Roorkee, under the project funded by Department of Science and Technology. The work presented in this paper is an outcome of the DST project, DST/23(483)/SU/2004. The author is sincerely thankful to anonymous referees whose valuable suggestions have improved the quality of this paper. The author also thanks Dr. V.K. Gupta, Editor, ISET Journal for his cooperation and support at the review stage of the work presented in this paper. The author kindly acknowledges the help of Kurukshetra University, Kurukshetra, in supporting the above-mentioned project.

REFERENCES

1. Anderson, J.G. and Hough, S.E. (1984). "A Model for the Shape of the Fourier Amplitude Spectrum of Acceleration at High Frequencies", Bulletin of the Seismological Society of America, Vol. 74, No. 5, pp. 1969-1993.
2. Atkinson, G.M. (1993). "Earthquake Source Spectra in Eastern North America", Bulletin of the Seismological Society of America, Vol. 83, No. 6, pp. 1778-1798.
3. Atkinson, G.M. and Boore, D.M. (1998). "Evaluation of Models for Earthquake Source Spectra in Eastern North America", Bulletin of the Seismological Society of America, Vol. 88, No. 4, pp. 917-934.
4. Atkinson, G.M. and Mereu, R.F. (1992). "The Shape of Ground Motion Attenuation Curves in Southeastern Canada", Bulletin of the Seismological Society of America, Vol. 82, No. 5, pp. 2014-2031.
5. Atkinson, G.M. and Silva, W. (1997). "An Empirical Study of Earthquake Source Spectra for California Earthquakes", Bulletin of the Seismological Society of America, Vol. 87, No. 1, pp. 97-113.
6. Atkinson, G.M. and Silva, W. (2000). "Stochastic Modeling of California Ground Motions", Bulletin of the Seismological Society of America, Vol. 90, No. 2, pp. 255-274.
7. Boatwright, J. and Choy, G.L. (1992). "Acceleration Source Spectra Anticipated for Large Earthquakes in Northeastern North America", Bulletin of the Seismological Society of America, Vol. 82, No. 2, pp. 660-682.
8. Boatwright, J., Fletcher, J.B. and Fumal, T.E. (1991). "A General Inversion Scheme for Source, Site, and Propagation Characteristics Using Multiply Recorded Sets of Moderate-Sized Earthquakes", Bulletin of the Seismological Society of America, Vol. 81, No. 5, pp. 1754-1782.
9. Bollinger, L., Avouac, J.P., Beyssac, O., Catlos, E.J., Harrison, T.M., Grove, M., Goffé, B. and Sapkota, S. (2004). "Thermal Structure and Exhumation History of the Lesser Himalaya in Central Nepal", Tectonics, Vol. 23, pp. 1-19.
10. Boore, D.M. (1983). "Stochastic Simulation of High-Frequency Ground Motions Based on Seismological Models of the Radiated Spectra", Bulletin of the Seismological Society of America, Vol. 73, No. 6A, pp. 1865-1894.
11. Boore, D.M. and Atkinson, G.M. (1987). "Stochastic Prediction of Ground Motion and Spectral Response Parameters at Hard-Rock Sites in Eastern North America", Bulletin of the Seismological Society of America, Vol. 77, No. 2, pp. 440-467.
12. Boore, D.M. and Atkinson, G.M. (1992). "Source Spectra for the 1988 Saguenay, Quebec, Earthquakes", Bulletin of the Seismological Society of America, Vol. 82, No. 2, pp. 683-719.
13. Brune, J.N. (1970). "Tectonic Stress and the Spectra of Seismic Shear Waves from Earthquakes", Journal of Geophysical Research, Vol. 75, pp. 4997-5009.
14. Brune, J.N. (1971). "Correction", Journal of Geophysical Research, Vol. 76, p. 5002.
15. Cattin, R., Martelet, G., Henry, P., Avouac, J.P., Diament, M. and Shakya, T.R. (2001). "Gravity Anomalies, Crustal Structure and Thermo-mechanical Support of the Himalaya of Central Nepal", Geophysical Journal International, Vol. 147, pp. 381-392.
16. Chandrasekaran, A.R. and Das, J.D. (1992). "Analysis of Strong Motion Accelerograms of Uttarkashi Earthquake of October 20, 1991", Bulletin of Indian Society of Earthquake Technology, Vol. 29, No. 1, pp. 35-55.

17. Fletcher, J.B. (1995). "Source Parameters and Crustal *Q* for Four Earthquakes in South Carolina", Seismological Research Letters, Vol. 66, No. 4, pp. 44-58.
18. Ganley, D.C. and Kanasewich, E.R. (1980). "Measurement of Absorption and Dispersion from Check Shot Surveys", Journal of Geophysical Research, Vol. 85, pp. 5219-5226.
19. Gupta, S.C., Singh, V.N. and Kumar, A. (1995). "Attenuation of Coda Waves in the Garhwal Himalaya, India", Physics of the Earth and Planetary Interiors, Vol. 87, No. 3, pp. 247-253.
20. Gusev, A.A. (1983). "Descriptive Statistical Model of Earthquake Source Radiation and its Application to an Estimation of Short Period Strong Motion", Geophysical Journal of Royal Astronomical Society, Vol. 74, No. 3, pp. 787-800.
21. Hamilton, E.L. (1972). "Compressional-Wave Attenuation in Marine Sediments", Geophysics, Vol. 37, No. 4, pp. 620-646.
22. Hamilton, E.L. (1976). "Sound Attenuation as a Function of Depth in the Sea Floor", The Journal of the Acoustical Society of America, Vol. 59, No. 3, pp. 528-535.
23. Hanks, T.C. (1982). "f_{max}.", Bulletin of the Seismological Society of America, Vol. 72, pp. 1867-1879.
24. Hauge, P.S. (1981). "Measurements of Attenuation from Vertical Seismic Profiles", Geophysics, Vol. 46, No. 11, pp. 1548-1558.
25. Hellweg, M., Spudich, P., Fletcher, J.B. and Baker, L.M. (1995). "Stability of Coda Q in the Region of Parkfield, California: View from the U.S. Geological Survey Parkfield Dense Seismograph Array", Journal of Geophysical Research, Vol. 100, No. B2, pp. 2089-2102.
26. Henry, P., Le Pichon, X. and Goffé, B. (1997). "Kinemetic, Thermal and Petrological Model of the Himalayas: Constraints Related to Metamorphism within the Underthrust Indian Crust and Topographic Elevation", Tectonophysics, Vol. 273, No. 1-2, pp. 31-56.
27. Hodges, K.V., Parrish, R.R. and Searle, M.P. (1996). "Tectonic Evolution of the Central Annapurna Range, Napalese Himalayas", Tectonics, Vol. 15, pp. 1264-1291.
28. Hudson, D.E. (1962). "Some Problems in the Application of Spectrum Techniques to Strong-Motion Earthquake Analysis", Bulletin of the Seismological Society of America, Vol. 52, No. 2, pp. 417-430.
29. Jain, A.K. and Chander, R. (1995). "Geodynamic Modelling of the Uttarkashi Earthquake of October 20, 1991" in "Uttarkashi Earthquake (edited by H.K. Gupta and G.D. Gupta)", Memoir No. 30, Geological Society of India, Kolkata.
30. Joshi, A. (2000). "Modelling of Rupture Planes for Peak Ground Accelerations and its Application to the Isoseismal Map of MMI Scale in Indian Region", Journal of Seismology, Vol. 4, No. 2, pp. 143-160.
31. Joshi, A. (2001). "Strong Motion Envelope Modelling of the Source of the Chamoli Earthquake of March 28, 1999 in the Garhwal Himalaya, India", Journal of Seismology, Vol. 5, No. 4, pp. 499-518.
32. Joshi, A., Singh, S. and Giroti, K. (2001). "The Simulation of Ground Motions Using Envelope Summations", Pure and Applied Geophysics, Vol. 158, No. 5-6, pp. 877-901.
33. Kanamori, H. and Stewart, G.S. (1978). "Seismological Aspects of the Guatemala Earthquake of February 4, 1976", Journal of Geophysical Research, Vol. 83, No. B7, pp. 3427-3434.
34. Kayal, J.R., Ghosh, B., Chakraborty, P. and De, R. (1995). "Aftershock Study of the Uttarkashi Earthquake of October 20, 1991 by a Temporary Microearthquake Network" in "Uttarkashi Earthquake (edited by H.K. Gupta and G.D. Gupta)", Memoir No. 30, Geological Society of India, Kolkata.
35. Khattri, K.N., Chander, R., Gaur, V.K., Sarkar, I. and Kumar, S. (1989). "New Seismological Results on the Tectonics of the Garhwal Himalaya", Proceedings of the Indian Academy of Sciences (Earth and Planetary sciences), Vol. 98, No. 1, pp. 91-109.
36. Knopoff, L. (1964). "*Q*", Reviews of Geophysics, Vol. 2, No. 4, pp. 625-660.
37. Kumar, D. and Khattri, K.N. (1999). "Average Intrinsic Q_s in the Crust and Uppermost 8 km of Mantle in the Ganga Plains, Bihar", Current Science, Vol. 77, No. 6, pp. 748-749.
38. Lancose, C. (1961). "Linear Differential Operators", Von Nostrand Reinhold, London, U.K.
39. Lee, V.W. and Trifunac, M.D. (1979). "Automatic Digitization and Processing of Strong Motion Accelerograms, Part II: Computer Processing of Accelerograms", Report 79-15, Department of Civil Engineering, University of Southern California, Los Angeles, U.S.A.
40. Le Fort, P. (1975). "Himalayas: The Collided Range. Present Knowledge of the Continental Arc", American Journal of Science, Vol. 275A, pp. 1-44.

41. Le Pichon, X., Henry, P. and Goffé, B. (1997). "Uplift of Tibet: From Eclogites to Granulites – Implications for the Andean Plateau and the Variscan Belt", Tectonophysics, Vol. 273, No. 1-2, pp. 57-76.
42. Mallet, F.R. (1874). "On the Geology and Mineral Resources of the Darjiling District and the Western Duars", Memoirs of Geological Survey of India, Vol. 11, pp. 1-94.
43. Mandal, P., Padhy, S., Rastogi, B.K., Satyanarayana, H.V.S., Kousalya, M., Vijayraghavan, R. and Srinivasan, A. (2001). "Aftershock Activity and Frequency-Dependent Low Coda Q_c in the Epicentral Region of the 1999 Chamoli Earthquake of M_w 6.4", Pure and Applied Geophysics, Vol. 158, No. 9-10, pp. 1719-1735.
44. McDonal, F.J., Angona, F.A., Mills, R.L., Sengbush, R.L., Van Nostrand, R.G. and White, J.E. (1958). "Attenuation of Shear and Compressional Waves in Pierre Shale", Geophysics, Vol. 23, No. 3, pp. 421-439.
45. Medlicott, H.B. (1864). "On the Geological Structure and Relations of the Southern Portion of the Himalayan Range between the River Ganges and Ravee", Memoirs of Geological Survey of India, Vol. 3, pp. 1-206.
46. Menke, W. (1984). "Geophysical Data Analysis: Discrete Inverse Theory", Academic Press Inc., New York, U.S.A.
47. Metcalfe, R.P. (1993). "Pressure, Temperature and Time Constraint on Metamorphism across the Main Central Thrust Zone and High Himalayan Slab in Garhwal Himalaya", in "Himalayan Tectonics (edited by P.J. Treloar and M.P. Searle)", Special Publication No. 74, Geological Society, London, U.K.
48. Oldham, R.D. (1883). "The Geology of Jaunsar and the Lower Himalayas", Records of the Geological Survey of India, Vol. 16, pp. 193-198.
49. Pandey, O.P. and Agrawal, P.K. (1999). "Lithospheric Mantle Deformation beneath the Indian Cratons", The Journal of Geology, Vol. 107, No. 6, pp. 683-692.
50. Papageorgiou, A.S. and Aki, K. (1983). "A Specific Barrier Model for the Quantitative Description of Inhomogeneous Faulting and the Prediction of Strong Ground Motion. I. Description of the Model", Bulletin of the Seismological Society of America, Vol. 73, No. 3, pp. 693-722.
51. Pêcher, A. (1975). "The Main Central Thrust of the Nepal Himalaya and the Related Metamorphism in the Modi-Khola Cross-Section (Annapurna Range)", Himalayan Geology, Vol. 5, pp. 115-132.
52. Press, W.H., Flannery, B.P., Teukolsky, S.A. and Vetterling, W.T. (1993). "Numerical Recipes in C: The Art of Scientific Computing", Cambridge University Press, Cambridge, U.K.
53. Rodriguez, M., Havskov, J. and Singh, S.K. (1983). "*Q* from Coda Waves near Petatlán, Guerrero, Mexico", Bulletin of the Seismological Society of America, Vol. 73, No. 1, pp. 321-326.
54. Roecker, S.W., Tucker, B., King, J. and Hatzfeld, D. (1982). "Estimates of *Q* in Central Asia as a Function of Frequency and Depth Using the Coda of Locally Recorded Earthquakes", Bulletin of the Seismological Society of America, Vol. 72, No. 1, pp. 129-149.
55. Rovelli, A. (1984). "Seismic Q for the Lithosphere of the Montenegro Region (Yugoslavia): Frequency, Depth and Time Windowing Effects", Physics of the Earth and Planetary Interiors, Vol. 34, No. 3, pp. 159-172.
56. Rudnicki, J.W. and Kanamori, H. (1981). "Effects of Fault Interaction on Moment, Stress Drop, and Strain Energy Release", Journal of Geophysical Research, Vol. 86, No. B3, pp. 1785-1793.
57. Savage, J. (1972). "Relation of Corner Frequency to Fault Dimension", Journal of Geophysical Research, Vol. 77, pp. 3788-3795.
58. Seeber, L. and Armbruster, J.G. (1984). "Some Elements of Continental Subduction along the Himalayan Front", Tectonophysics, Vol. 105, No. 1-4, pp. 263-278.
59. Sharma, M.L. and Wason, H.R. (1994). "Occurrence of Low Stress Drop Earthquakes in the Garhwal Himalaya Region", Physics of the Earth and Planetary Interiors, Vol. 85, pp. 265-272.
60. Singh, S.K., Apsel, R.J., Fried, J. and Brune, J.N. (1982). "Spectral Attenuation of SH-Waves along the Imperial Fault," Bulletin of the Seismological Society of America, Vol. 72, No. 6, pp. 2003-2016.
61. Singh, S.K., Mohanty, W.K., Bansal, B.K. and Roonwal, G.S. (2002). "Ground Motion in Delhi from Future Large/Great Earthquakes in the Central Seismic Gap of the Himalayan Arc", Bulletin of the Seismological Society of America, Vol. 92, No. 2, pp. 555-569.

62. Sriram, V. and Khattri, K.N. (1997). “A Study of Source Spectrum, Site Amplification Functions, Response Spectra, Fourier Spectra, and Peak Ground Accelerations from the Strong Ground Motion Data of the 1991 Uttarkashi Earthquake”, Current Science, Vol. 72, No. 10, pp. 728-740.
63. Stephenson, B.J., Waters, D.J. and Searle, M.P. (2000). “Inverted Metamorphism and the Main Central Thrust: Field Relations and Thermobarometric Constraints from the Kishtwar Window NW Indian Himalaya”, Journal of Metamorphic Geology, Vol. 18, No. 5, pp. 571-590.
64. Thakur, V.C. and Kumar, S. (2002). “Seismotectonic of Chamoli Earthquake of March 29, 1999 and Earthquake Hazard Assessment of Garhwal-Kumaun Region, NW Himalaya”, Himalayan Geology, Vol. 23, No. 1-2, pp. 113-119.
65. Thouvenot, F. (1983). “Frequency Dependence of the Quality Factor in the Upper Crust: A Deep Seismic Sounding Approach”, Geophysical Journal of Royal Astronomical Society, Vol. 73, pp. 427-447.
66. Tullos, F.N. and Reid, A.C. (1969). “Seismic Attenuation of Gulf Coast Sediments”, Geophysics, Vol. 34, No. 4, pp. 516-528.
67. Trifunac, M.D. (1972a). “Stress Estimates for the San Fernando, California, Earthquake of February 9, 1971: Main Event and Thirteen Aftershocks”, Bulletin of the Seismological Society of America, Vol. 62, No. 3, pp. 721-750.
68. Trifunac, M.D. (1972b). “Tectonic Stress and the Source Mechanism of the Imperial Valley, California, Earthquake of 1940”, Bulletin of the Seismological Society of America, Vol. 62, No. 5, pp. 1283-1302.
69. Trifunac, M.D. (1994). “Fourier Amplitude Spectra of Strong Motion Acceleration: Extension to High and Low Frequencies”, Earthquake Engineering and Structural Dynamics, Vol. 23, No. 4, pp. 389-411.
70. Trifunac, M.D. and Lee, V.W. (1973). “Routine Computer Processing of Strong-Motion Accelerograms”, Report EERL 73-03, California Institute of Technology, Pasadena, U.S.A.
71. Yu, G., Khattri, K.N., Anderson, J.G., Brune, J.N. and Zeng, Y. (1995). “Strong Ground Motion from the Uttarkashi, Himalaya, India, Earthquake: Comparison of Observations with Synthetics Using the Composite Source Model”, Bulletin of the Seismological Society of America, Vol. 85, No. 1, pp. 31-50.